Journal of Environmental Management 301 (2022) 113750

Contents lists available at ScienceDirect

Journal of Environmental Management

journal homepage: www.elsevier.com/locate/jenvman

Blue-green roofs with forecast-based operation to reduce the impact of weather extremes

Tim Busker [a,*], Hans de Moel [a], Toon Haer [a], Maurice Schmeits [b,a], Bart van den Hurk [c,a], Kira Myers [a], Dirk Gijsbert Cirkel [d], Jeroen Aerts [a,c]

[a] Institute for Environmental Studies (IVM), Vrije Universiteit Amsterdam, Amsterdam, 1081 HV, the Netherlands
[b] Royal Netherlands Meteorological Institute (KNMI), De Bilt, 3731 GA, the Netherlands
[c] Deltares, Delft, 2600 MH, the Netherlands
[d] KWR Water Research Institute, Nieuwegein, 3433 PE, the Netherlands

ARTICLE INFO

Keywords:
Green roof
Blue-green roof
Stormwater management
Flood risk
Heat stress
Climate adaptation

ABSTRACT

Conventional green roofs have often been criticised for their limited water buffer capacity during extreme rainfall events and for their susceptibility to droughts when additional irrigation is unavailable. One solution to these challenges is to create an extra blue water retention layer underneath the green layer. Blue-green roofs allow more stormwater to be stored, and the reservoir can act as a water source for the green layer throughout capillary rises. An automated valve regulates the water level of the system. It can be opened to drain water when extreme precipitation is expected. Therefore, the water buffer capacity of the system during extreme rainfall events can be maximised by integrating precipitation forecasts as triggers for the operation of the valve. However, the added value of this forecast-based operation is yet unknown. Accordingly, in this study, we design and evaluate a hydrological blue-green roof model that utilises precipitation forecasts. We test its performance to capture (extreme) precipitation and to increase evapotranspiration and evaporative cooling under a variety of precipitation forecast-based decision rules. We show that blue-green roofs can capture between 70 % and 97 % of extreme precipitation (>20 mm/h) when set to anticipate ensemble precipitation forecasts from the European Centre for Medium-Range Weather Forecasts (ECMWF). This capture ratio is considerably higher than that of a conventional green roof without extra water retention (12 %) or that of a blue-green roof that does not use forecast information (i.e., valve always closed; 59 %). Moreover, blue-green roofs allow for high evapotranspiration rates relative to potential evapotranspiration on hot summer days (around 70 %), which is higher than from conventional green roofs (30 %). This serves to underscore the higher capacity of blue-green roofs to reduce heat stress. Using the city of Amsterdam as a case study, we show the high upscaling potential of the concept: on average, potentially suitable flat roofs cover 13.3 % of the total area of the catchments that are susceptible to pluvial flood risk. If the 90th percentile of the ECMWF forecast is used, an 84 % rainfall capture ratio can translate into capturing 11 % of rainfall in flood-prone urban catchments in Amsterdam.

1. Introduction

Research has shown that the intensity and frequency of heavy precipitation events increased since the 1950s over most land areas with sufficient observations (IPCC, 2021). Anthropogenic greenhouse gas emissions are likely the main driver behind this observed trend (IPCC, 2021). Research on national climate scenarios in the Netherlands highlights a consistent change, with an increase in extreme precipitation events in both summer and winter as global warming levels rise (Van den Hurk et al., 2014). Combined with rapid urbanisation and the densification of exposed assets, these changes have contributed to a higher risk of pluvial flood damage in Europe (Skougaard Kaspersen et al., 2017). The impact of these changes in rainfall patterns for Western Europe became clear in the summer of 2021: 100–150 mm of rainfall in 24 h caused unprecedented floods in multiple parts of Germany, Austria, Belgium and the Netherlands (World Meteorological Organization (WMO), 2021). Just some weeks earlier, the Pacific Northwest areas of the United States and Canada faced an extraordinary heatwave, with

* Corresponding author.
E-mail address: tim.busker@vu.nl (T. Busker).

https://doi.org/10.1016/j.jenvman.2021.113750
Received 20 June 2021; Received in revised form 10 September 2021; Accepted 11 September 2021
Available online 28 September 2021

historical records exceeded by several degrees Celsius (WMO, 2021). Scientists found this event would have been virtually impossible without human-induced global warming (World Weather Attribution (WWA, 2021)). The climate is already becoming more erratic; a trend which will only exacerbate over coming decades (IPCC, 2021). These extremes can also strike large European metropoles, like Amsterdam, where climate adaptation is challenging but crucial.

It is widely accepted that green infrastructure (e.g. parks, green roofs, etc.) decreases urban pluvial flood risk by boosting storage capacity, infiltration and evapotranspiration, resulting in less surface runoff (World Wildlife Fund (WWF), 2016). Green infrastructure provides a wide range of additional benefits. A large body of studies now emphasizes the significant mental (e.g. happiness and stress levels) and physical health benefits green infrastructure can generate in the built environment (Kellert and Calabrese, 2015; Tzoulas et al., 2007; van den Berg et al., 2015). Green infrastructure can also reduce indoor energy consumption (La Roche and Berardi, 2014; Razzaghmanesh et al., 2016) and the Urban Heat Island (UHI) effect (Aflaki et al., 2017; Mohajerani et al., 2017). Blue infrastructure (e.g., detention basins or retention ponds) can also store excess rainwater and thus attenuate stormwater concerns. Instead of opting for either a green or a blue solution, recent efforts have combined the benefits of the two solutions in what has come to be called “blue-green infrastructure”. This development resulted in the emergence of several initiatives to reduce flood risk, including the Sponge City concept in China, the Low-Impact Development approach in the United States and the Blue-Green Cities concept in the United Kingdom (Chan et al., 2018).

The implementation of green infrastructure in metropoles is often limited by the available space, and retrofitting existing urban landscapes is often prohibitively expensive. Urban development therefore benefits from multifunctional solutions and integrating green infrastructure into the existing urban landscape. This makes green roofs often attractive solutions. They decrease indoor temperatures and heat stress on hot summer days and provide extra insulation in winter (Razzaghmanesh et al., 2016). Moreover, modelling studies indicate strongly that green roofs can contribute considerably to the reduction of the UHI effect, especially on hot summer days (Alexandri and Jones, 2008; Mohajerani et al., 2017; Razzaghmanesh et al., 2016). Despite these benefits, the water buffer capacity of green roofs during extreme precipitation events has been shown to be limited, particularly when the soil is already saturated (Huang et al., 2020; Lee et al., 2015; Viavattene and Ellis, 2013; Yao et al., 2020; Zhang et al., 2021). Zhang et al. (2021) found that green roofs with different substrate characteristics have retention rates of only 5–15 % in extreme rainfall events with a return period between 5 and 50 years.

To circumvent this limitation, recent research has begun exploring the benefits of combining both solutions through blue-green roofs, that is, green roofs with blue water retention layers (Fig. 2a). These structures can cope with extreme hydrological events better because the water level in the blue layer can be regulated. Water can be drained if heavy precipitation is forecast, or it can be stored to irrigate the green layer during hot and dry periods (RESILIO, 2020). Optimising the effectiveness and the operation of the valve that regulates the water level in the blue layer is a key challenge in managing these blue-green roofs. A high water level is desirable to increase the supply of water to plants during dry periods and to increase evaporative cooling on hot summer days. However, a low water level is best just before extreme rainfall events because it can ensure sufficient buffer capacity and minimise roof runoff. For this mode of operation to be achieved, it is necessary to anticipate precipitation and to optimize the buffer capacity of the blue layer through the controlled release of water prior to rainfall events. However, despite improvements in precipitation intensity forecast, forecasting local extreme precipitation events is still very challenging, even with non-hydrostatic numerical weather prediction (NWP) models (Manola et al., 2018). Furthermore, forecast accuracy generally decreases for higher-intensity events, such as the convective summer precipitation that occurs frequently in the Netherlands, which are typically spatially limited (Imhoff et al., 2020). A forecast-based action system for blue-green roofs should therefore account for such uncertainties.

The literature on blue-green roofs has focused on technical construction (Andenæs et al., 2021; Skjeldrum and Kvande, 2017) and stormwater management (Pelorosso et al., 2021; Shafique et al., 2016). However, none of these studies focus on the added value of using weather forecast information to increase the effectiveness of blue-green roofs further. Therefore, the aim of this study is to assess the effectiveness of blue-green roofs in reducing peak discharge by utilising a smart forecast-based action system which triggers roof drainage from the blue layer. To this end, we combine a conceptual hydrological model that simulates the main hydrological processes in a blue-green roof with ensemble-based precipitation forecasts. The adoption of the latter enables us to assess the added value of a variety of forecast-based blue--green roof operations.

The blue-green roof concept will be explored further in the section on methods. That part is followed by the main research framework, input data and an overview of the hydrological model, including the integration of forecast information (Section 2). In the results section (Section 3), we will evaluate the main performance indicators for the different forecast-based drainage strategies. The results will be discussed in Section 4 and summarised in the conclusion (Section 5).

2. Methods

2.1. Blue-green roofs

In July 2011, the city of Copenhagen faced a rainstorm event of unparalleled proportions, with 150 mm of rain in less than 2 h. This storm was a wake-up call for the city of Amsterdam and prompted the initiation of the Amsterdam Rainproof Program in January 2014. In line with the goals of the program, the city has initiated pilots and research on blue-green roofs through the Smartroof 2.0 initiative and, more recently, the RESILIO project (RESILIO, 2020). The blue layer of those roofs is situated underneath the green soil layer and above the roof deck. It consists of plastic crates that are 8 cm deep, which create additional storage capacity for excess rainwater (Fig. 2a). A water- and root-proof layer is situated underneath the blue layer to prevent leakage and damage from plant roots (Fig. 2a). Moreover, the existing roof deck needs to be strengthened with an extra cement layer, and waterproof and root-resistant bitumen. Plants in the green layer can extract water from the blue layer through capillary fibre cylinders, which reduces the need for irrigation and increases the resilience of the plant layer during meteorological droughts (Cirkel et al., 2018). Furthermore, water in the blue layer can be released using a smart valve (The Smart Drop®) that was developed by the Dutch company MetroPolder (MetroPolder company, 2021a). The automated smart valve can be fed weather forecast information to respond to extreme precipitation or drought forecasts. For example, water can be released from the blue layer when an extreme precipitation event is forecast, creating the necessary buffer capacity to capture the rainfall. Conversely, when a dry period is forecast, the valve could be closed in advance to keep the water level as high as possible in an attempt to prevent vegetation from drying. Although the operational system to connect the valve to weather forecasts is present, the effectiveness and optimal configuration of this forecast-based operation is still unknown.

2.2. Research framework

Fig. 1 shows the overall approach of this research to testing the performance of a synthetic blue-green roof. The approach is based on ensemble precipitation forecasting data from the European Centre for Medium-Range Weather Forecasts (ECMWF). After pre-processing, these ensemble data were used as an input for a hydrological model that

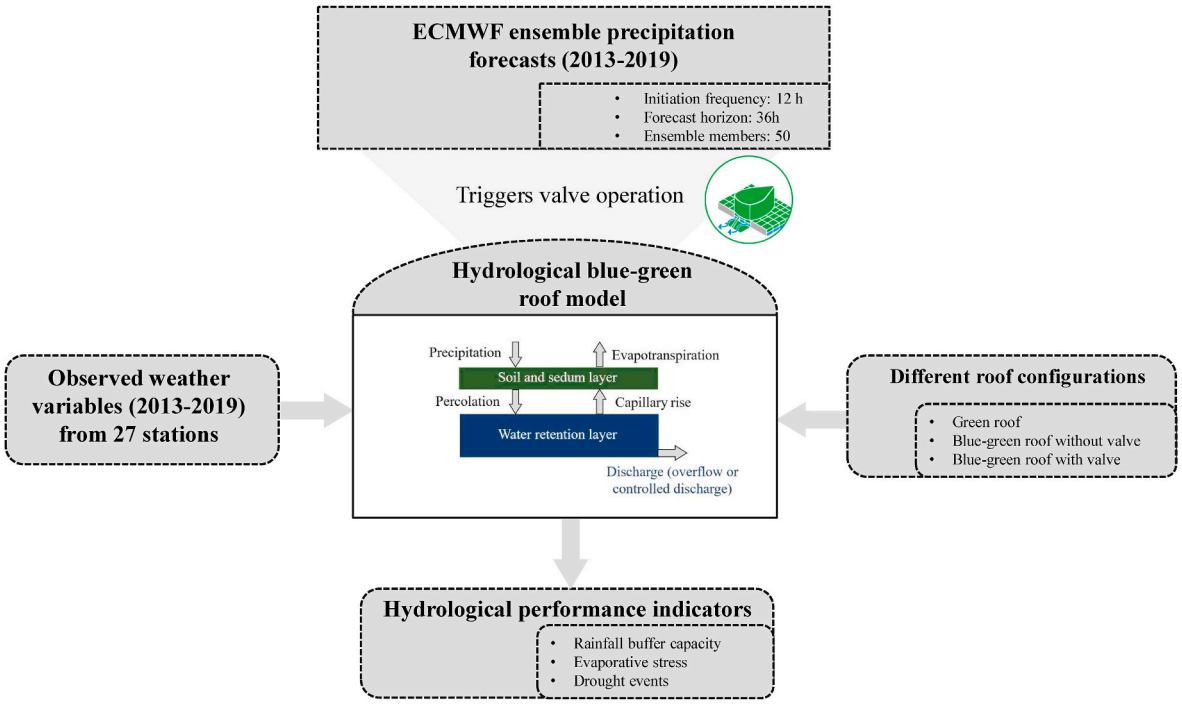

Fig. 1. Framework of the research methodology, including inputs to the hydrological model and the three performance indicators used in the evaluation.

simulates the hydrological flows of a blue-green roof. Different forecast-based drainage strategies (see Table 1) were developed to trigger opening of the smart valve and to drain water from the blue layer based on ensemble precipitation forecasts. We also formulated hydrological performance indicators to assess the different early-drainage strategies. The hydrological model was ran with weather data from 27 automatic weather stations in the Netherlands (2013–2019). Evaluating the model with data from 27 different locations ensures that a sufficient number of extreme rainfall events are included in the analysis and therefore limits the uncertainty of the hydrological performance indicators.

2.3. Data

2.3.1. ECWMF precipitation ensemble forecasts

For the forecast-based action system, we used probabilistic forecast information from ECMWF, which we downloaded by using the web API (ECMWF, 2021). For the years 2017, 2018 and 2019, we downloaded forecasts from The International Grand Global Ensemble (TIGGE) database (Bougeault et al., 2010; Swinbank et al., 2016). The TIGGE database is a global historical archive of operational ensemble forecasts from 10 NWP centres. The records start from October 2006. As data for some months were unavailable in the TIGGE dataset, we downloaded ensemble precipitation forecasts for the years between 2013 and 2016 from the ECMWF MARS data archive. The TIGGE ECWMF ensemble precipitation forecasts contain the same type of data as the ECMWF MARS forecasts, which allowed the two data sources to be combined. This combination yielded seven years of continuous historical ensemble precipitation forecasts with 50 perturbed ensemble members of which we used forecasts with a maximum lead time of 36 h (see Fig. S2). The ECMWF ensemble forecasts are initiated twice a day, providing continuous accumulated precipitation forecasts with a 6-h time step (i.e., 0–6 h, 0–12 h, 0–18 h, 0–24 h, 0–30 h, 0–36 h). We converted them to 6-h accumulations. The horizontal resolution of the ECMWF ensemble precipitation forecasts was approximately 35 km from January 2010 to March 2016. Thereafter, it increased to approximately 18 km on a cubic-octahedral grid, up to a lead time of 15 days (Buizza and Richardson, 2017). Since ECMWF reforecast runs on the current resolution are performed twice a week rather than of twice a day (and with only 10 perturbed ensemble members), we chose to use the operational data record with these two resolutions.

2.3.2. Meteorological observations

To run the hydrological model on as many locations as possible, we used weather data from all 27 KNMI weather stations in the Netherlands for which continuous data was available over the seven years (2013–2019) analysed in this study (Fig. S1). We downloaded data for the 2013–2019 period for each of these stations (KNMI, 2021). We sampled all 27 locations to increase the statistical robustness of the output of the model, which is especially important for extreme rainfall (>20 mm) events with a low return period. Six out of 27 stations did not record any extreme events, and the stations with extreme rainfall recorded 1–5 events each. The meteorological data cover hourly precipitation observations and daily meteorological variables. The latter, namely global radiation, mean windspeed, mean, minimum and maximum temperature, and minimum and maximum relative humidity, were used for the evaporation segment of the hydrological model. The hourly precipitation observations are used as input to the blue-green roof in the hydrological model on every 10-min time step. They are also used to generate a perfect forecast in the 'perfect_forecast' drainage strategy (see Table 1).

2.4. The hydrological model

We developed the hydrological model in question to simulate the forecast-based operation of blue-green roofs. Our analysis is premised on the conventional recharge model presented by Ireson and Butler (2013) and the blue-green roof model that was developed by Cirkel et al. (2018). Our two-layered bucket model simulates the main hydrological fluxes on blue-green roofs, namely precipitation, evapotranspiration, capillary rise, percolation, controlled discharge and overflow (see Fig. 2b). Every 10 min, these flows result in a new water level in the green and blue layers. We simulated one of the RESILIO pilot roofs with a size of 480 m^2 and used the same configuration (water capacity and vegetation type) as the roofs that had been implemented in that project. The green layer consists of sedum vegetation and a 60-mm deep substrate. Sedum is commonly seen on green roofs, and the majority of the

species in commercially available sedum mix blankets and plugs (e.g., Sedum album, Sedum acre, Sedum kamschaticum) exhibit a water status-dependent metabolism as an adaptation to droughts (Cirkel et al., 2018; Gravatt and Martin, 1992; Kuronuma and Watanabe, 2017; Pilon-Smits et al., 1991). Typically, the metabolism of sedum species is of the C3 pathway. Transpiration rates are relatively high when water is available, but sedum can switch to crassulacean acid metabolism (CAM) when water becomes scarce. Therefore, sedum species still provide considerable daytime evaporative cooling when the supply of water is abundant. The water storage capacity of the green layer is 12 mm on average (20 % of the 60 mm substrate; (MetroPolder company, 2021b)). The blue layer has a capacity of 71 mm, which is lower than the height of the crates (80 mm) due to the capillary rise cylinders (MetroPolder company, 2021b). The blue and green layers are connected through capillary rise and percolation. Percolation from the green layer into the blue layer occurs when the green layer becomes saturated during precipitation. Capillary rise occurs when the green layer is not saturated, provided that water is available in the blue layer. The blue layer can discharge water onto the stormwater drainage system through overflow or through controlled drainage. Overflow to the city drainage system occurs without any intervention when the capacity of the blue layer (71 mm) is exceeded during rainfall (Fig. 2b, red line in the blue layer). To prevent uncontrolled overflow, we apply regulated forecast-based drainage by operating the smart valve. The valve has a width of 12 cm. We simulated discharge through the valve in line with the Poleni equation (Indlekofer and Rouve, 1975).

We used the method of Cirkel et al. (2018) to estimate daily potential evapotranspiration (PET) and actual evapotranspiration (ETa) from blue-green roofs with a sedum plant cover, based on the water content in the blue layer and the green layer and daily potential evapotranspiration (PET). Daily PET values were calculated using the Penman-Monteith equation (Allen et al., 1998; Monteith and Unsworth, 2013; Penman, 1948) and daily observations from each of the selected KNMI weather stations. ETa is based on the water content of the green layer and daily PET values, and it is updated every 10 min. Cirkel et al. (2018) methodology assumes that ETa is equal to PET when the amount of water in the green layer exceeds 10 mm (Fig. 2b, red line in the green layer). For lower water contents, ETa decreases linearly with water content. As the green layer only begins to dry if the blue layer is empty, ETa only decreases relative to PET if the blue layer is empty and ETa from the green layer exceeds precipitation.

2.5. Early drainage based on ECMWF forecasts

Given a roof size of 480 m^2, and a smart valve width of 12 cm, it takes approximately 24 h to drain the blue layer completely by opening the smart valve. ECMWF issues operational ensemble forecasts every 12 h. To ensure that 24 h are always available to drain the blue layer, we chose a forecast horizon of 36 h. We ran the hydrological model twice a day with updated ECMWF forecasts to determine whether the forecast precipitation amount would exceed the system capacity of 71 mm, that is, whether unwanted overflow would occur. The valve only opens in these cases that overflow is forecast. Table 1 (and Fig. S2) shows the use of this ensemble forecast information. An ensemble distribution of 50 members is available for each 6-h forecast accumulation period in the 36-h forecast horizon. Precipitation intensity percentiles are derived from this ensemble after ranking the 50 ensemble members from smallest to largest. We used six different percentile variations: the 30th, 60th, 90th and the 99th percentile as well as increasing and decreasing percentiles with lead time (Table 1 and Fig. S2). The following strategy names were adopted: 'per_30', 'per_60', 'per_90', 'per_99', 'per_increasing' and 'per_decreasing'. The valve opens, that is, controlled drainage starts, when the total precipitation amount indicated by these percentiles over the 36-h forecast horizon exceeds the current capacity of the blue layer (Fig. S2). However, the valve never opens at moments that it is already raining.

The 'per_X' strategies drain fixed percentiles for all lead times (30th, 60th, 90th or 99th). The 'per_increasing' strategy increases the corresponding percentile for each 12-h lead time interval, varying from the 30th percentile for the period between 0 and 12 h to the 60th percentile for the period between 12 and 24 h and the 90th percentile for the period between 24 and 36 h (Table 1 and Fig. S2). The rationale behind this strategy is that for longer lead times, heavy precipitation events will generally only be predicted by a few extreme ensemble members. The 90th percentile therefore allows these extreme events to be detected in an early stage. A new ECMWF run is initiated every 12 h, and it generates a new drainage decision point. A single heavy precipitation event forecast with a lead time of between 30 and 36 h can never lead to the full capacity of the blue layer (71 mm) being drained because 12 h are insufficient to drain that amount of water. Another extreme forecast is needed in the subsequent forecast run (12 h later) for the full capacity of the roof to be drained. This strategy is a desired system configuration as it may compensate for early-forecast false alarms by reconsidering the

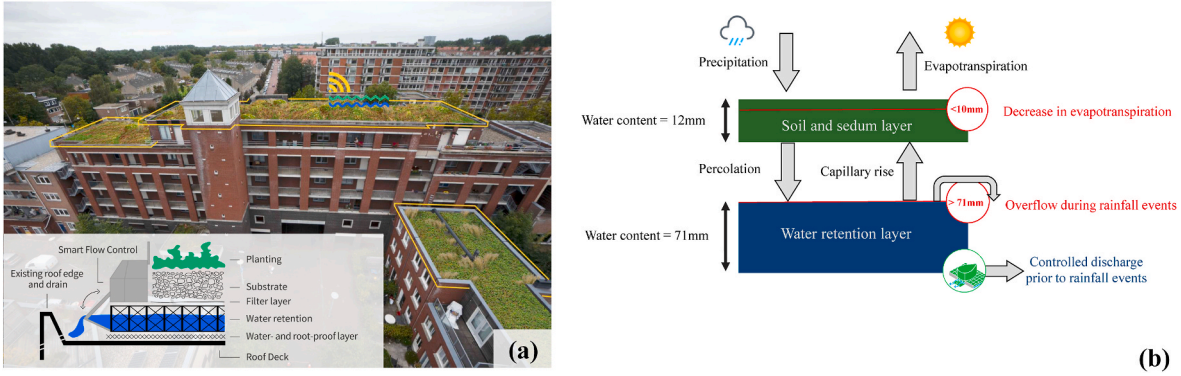

Fig. 2. Panel a: An illustration of the blue-green roof concept. The roof that is shown is an artist impression of a pilot roof realised as part of the RESILIO project in Amsterdam (RESILIO, 2020). The visualisation on the bottom left shows the different roof layers. **Panel b**: The configuration of these roofs in the hydrological model. The red lines show the water content thresholds for which exceedance produces undesired outcomes (overflow for the blue layer, reduced ETa for the green layer). (For interpretation of the references to colour in this figure legend, the reader is referred to the Web version of this article.)

Table 1
An overview of the different strategies assessed in this study, including the forecast-based drainage strategies.

	Strategy description		Strategy name
No drainage	Traditional green roof		Green_roof
	Blue-green roof without drainage		BG_bucket
Forecast-based drainage	Trigger to open valve: Precipitation forecast exceeds blue layer capacity (i.e., overflow is predicted), according to	ECMWF's X^{th} percentile	Per_X
		ECMWF's X^{th} percentile and decrease percentile with lead time: - 0-12h: 90th percentile - 12-24h: 60th percentile - 24-36h: 30th percentile	Per_decreasing
		ECMWF's X^{th} percentile and increase percentile with lead time: - 0-12h: 30th percentile - 12-24h: 60th percentile - 24-36h: 90th percentile	Per_increasing
		A perfect forecast: observed precipitation for the next 36h	Perfect_forecast

drainage in the subsequent forecast. The 'per_decreasing' strategy, conversely, tests whether high percentiles for short lead times improve the operation of the roof.

We compared the precipitation forecast-based roof operation with several benchmarks: a perfect forecast based on future observations ('perfect_forecast'), a blue-green roof without any drainage ('BG_bucket') and a traditional green roof without a blue layer ('green_roof'; Table 1).

2.6. Roof performance indicators

We formulated hydrological performance indicators to test the extent to which the different early action strategies enable the attainment of the most important objectives of a blue-green roof: (1) maximising buffer capacity during rainfall events and therefore minimising unwanted overflow and the resultant urban flooding; (2) maximising the overall water level to maximise ETa and the resultant evaporative cooling; and (3) minimising vegetation drought stress and mortality.

$$Performance_{\text{buffer}} = \frac{Total\ rainfall\ captured\ (mm)}{Total\ rainfall\ (mm)} * 100 \quad (1)$$

$$Performance_{\text{ET}} = \frac{ETa\ (mm)}{PET\ (mm)} * 100 \quad (2)$$

$$Performance_{\text{droughts}} = \left(1 - \frac{\#\ drought\ events}{\#\ years\ analyzed}\right) * 100 \quad (3)$$

$Performance_{\text{buffer}}$ (Eq. (1)) yields the percentage of all precipitation that the blue-green roof captures. Every deviation below 100 denotes the occurrence of unwanted overflow. $Performance_{\text{ET}}$ (Eq. (2)) is very similar to the crop water stress indicator defined by Jackson et al. (1981). It expresses the amount of ETa relative to PET and is therefore an indicator of water stress and evaporative cooling. $Performance_{\text{droughts}}$ (Eq. (3)) minimises the number of cases in which water is depleted from the green layer over a long period. This green layer drought is defined as a 28-day period with <10 mm of water in the green layer. This threshold has been found to be the critical: once it is exceeded, a sedum plant with a substrate depth of 6 cm requires additional irrigation to continue growing and to stay green (Van Woert et al., 2005). Inevitably, a trade-off exists between the performance indicator of Eq. (1) on the one hand and those of Eq. (2) and Eq. (3) on the other: for buffer capacity to be optimised, the blue layer needs to be as empty as possible, but a full green layer is optimal for cooling and drought resistance. False heavy rainfall alarms may drain blue-layer water unnecessarily and lower the performance indicators measured by Eq. (2) and Eq. (3). Conversely, overly conservative draining may cause insufficient rainwater storage capacity during extreme events and result in otherwise preventable overflow. The optimal early-drainage strategy and indicator values ultimately depend on the balance between the costs of additional overflow (and the corresponding increase in pluvial flood risk) and those of lower evaporation (and the corresponding decrease in evaporative cooling).

2.7. Case-study application: suitability analysis in Amsterdam

With a population of almost 900,000 inhabitants, Amsterdam is the capital of the Netherlands and its largest city. Situated near the North Sea, Amsterdam receives year-round rainfall, mainly brought by south-westerly winds. The city has faced several extreme precipitation events, such as the cloudburst of July 28, 2014, which saw record intensities of 140 mm/day (Manola et al., 2018). As the sewerage system in the city was designed to cope only with 20 mm/h, the 2014 cloudburst resulted in the inundation of major streets (Redactie Rainproof, 2020). According to Van Oldenborgh and Lenderink (2014), the return period of such an event in the country is between five and 15 years.

To gauge the city-wide prospects of blue-green roofs, we estimated their potential surface area for different parts of the city ('urban catchments') that are prone to pluvial flooding. A roof is classified as suitable if it is flat and larger than 200 m^2 (blue-green roofs need to have a size of at least 200 m^2 to be economically viable). We used a dataset from Amsterdam's public water utility company, Waternet. The dataset contains a classification of flat roofs in Amsterdam (Waternet and Tauw, 2017). A roof is classified as flat if more than 60 % of its surface has a

slope of less than 11°. Roof slopes for each building were calculated using raster elevation data with a 0.5 m horizontal resolution, measured using airborne laser altimetry (AHN3; Dutch government, 2017). Building location and shape were extracted from the *Basisregistratie Adressen en Gebouwen* (BAG) dataset (Dutch government, 2021). As some flat building blocks contained many small individual properties (<200 m^2), we used the *K*-means multivariate clustering algorithm (ESRI, 2021) to detect neighbouring flat roofs with a similar elevation. We combined neighbouring roofs that belonged to the same cluster and whose elevation differences did not exceed 0.5 m. Whenever these combined polygons became larger than 200 m^2, we included them in the dataset as well. Subsequently, we estimated the share of extreme precipitation (>20 mm/h) that can be captured by these potentially suitable roofs in urban catchments that are exposed to flood risk, say because of bottlenecks in the drainage system. As the average capacity of the drainage system in Amsterdam is also 20 mm/h, this share of rainfall captured gives an indication of the magnitude of flood risk reduction in the urban catchments. Our estimate is premised on the assumption that the average extreme rainfall capture ratio ($Performance_{buffer}$) for the 27 locations that are assessed in this study is a good approximation of the real average capture ratio of a single blue-green roof in Amsterdam.

3. Results

3.1. An illustrative example: time series of a modelled blue-green roof

We used 27 different weather stations to simulate the operation of blue-green roofs. Here, we showcase the roof-scale simulation which uses the hydrological model that is driven by ECMWF precipitation forecasts and observations from the weather station at Schiphol Airport. Fig. 3 shows the precipitation time series (observed and forecast; the two upper panels), water level (in the blue and green layer; third panel) and roof discharge (controlled drainage and overflow; lower panel) for one synthetic roof over the 2013–2019 period when the 'per_90' strategy is used. This illustrates how the blue and green layers react to dry spells and rainfall events of varying magnitude. A distinct characteristic of blue-green roofs in the Netherlands is that in summer, average water levels are comparatively low. This is advantageous for buffering storm water as extreme cloudbursts in the region occur due to deep convection in hot summers. At the Schiphol Airport station, two extreme rainfall events are highlighted in the time series. The two were also predicted by ECMWF, although their magnitude was underestimated. Simulations show that the first of these events, in 2014, had a sufficiently low water level at the start of the event to avoid unwanted overflow. The second one, in 2016, however, did result in overflow as a result of an underestimation in the overflow prediction by the ECMWF 90th percentile. Only one 28-day drought event (<10 mm water in the green layer) occurs in the time series. It dates from the extremely dry summer of 2018. This said, other dry spells (2013, 2015) are also in evidence. Water levels during the summer of 2016 were notably high.

3.2. Hydrological performance of the modelled roofs

3.2.1. Overall hydrological performance

We tested the overall hydrological performance of the roofs on the locations of the 27 weather stations (Fig. 4). The performance indicators are depicted in boxplots and representing the distribution of accumulated values over the seven years under observation. Without the blue layer, the green layer would store approximately 30 % of the total precipitation (leftmost blue box in Fig. 4), with the other 70 % being uncontrolled overflow. When the blue layer is added without any controlled drainage ('BG_bucket'), the capture ratio increases to approximately 50 %. The addition of the smart control improves performance considerably, with values in excess of 90 % under most

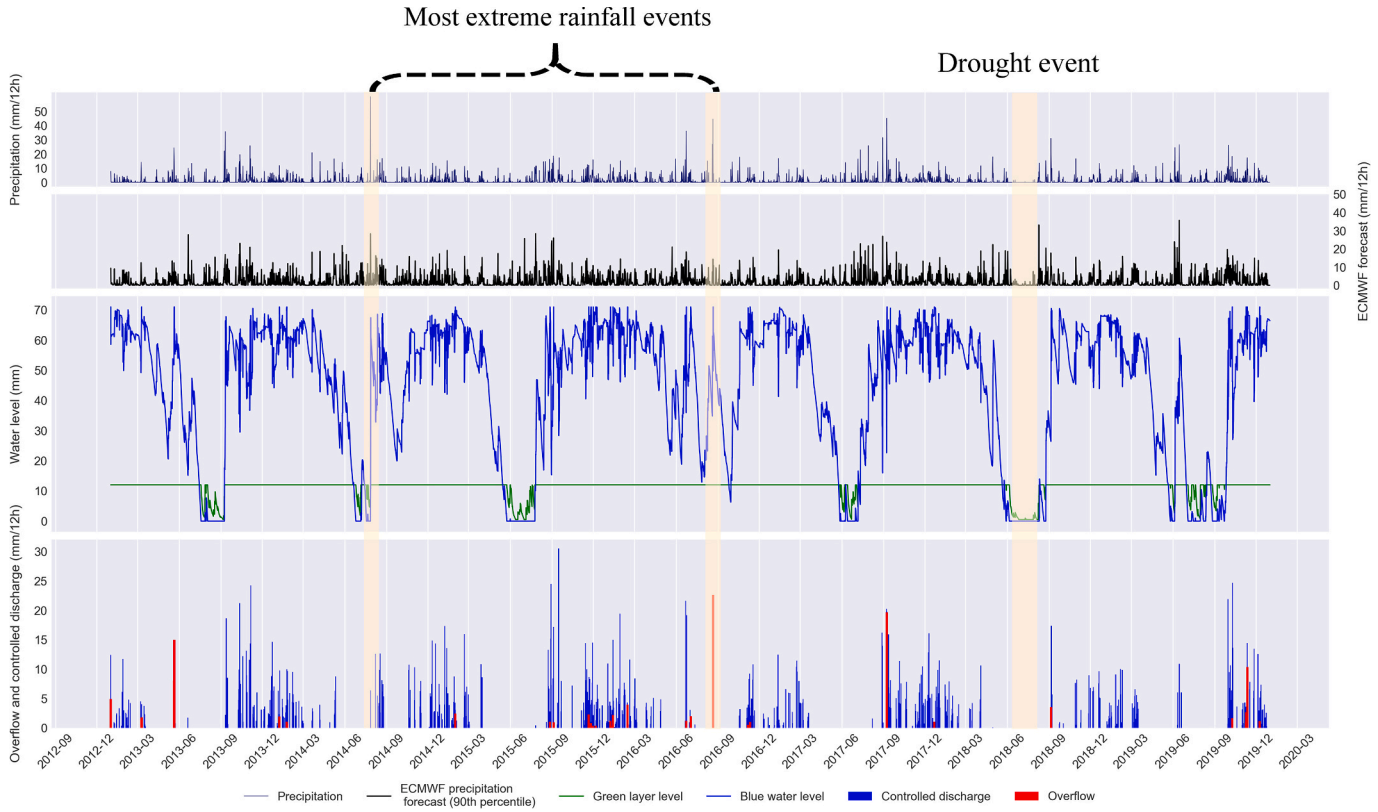

Fig. 3. Time series of observed and forecast precipitation (upper two panels), water levels in the blue and green layer (third panel) and overflow and controlled discharge (lower panel) using the 'per_90' strategy for the weather station on Schiphol Airport. Two extreme rainfall events and one 28-day drought event are highlighted. (For interpretation of the references to colour in this figure legend, the reader is referred to the Web version of this article.)

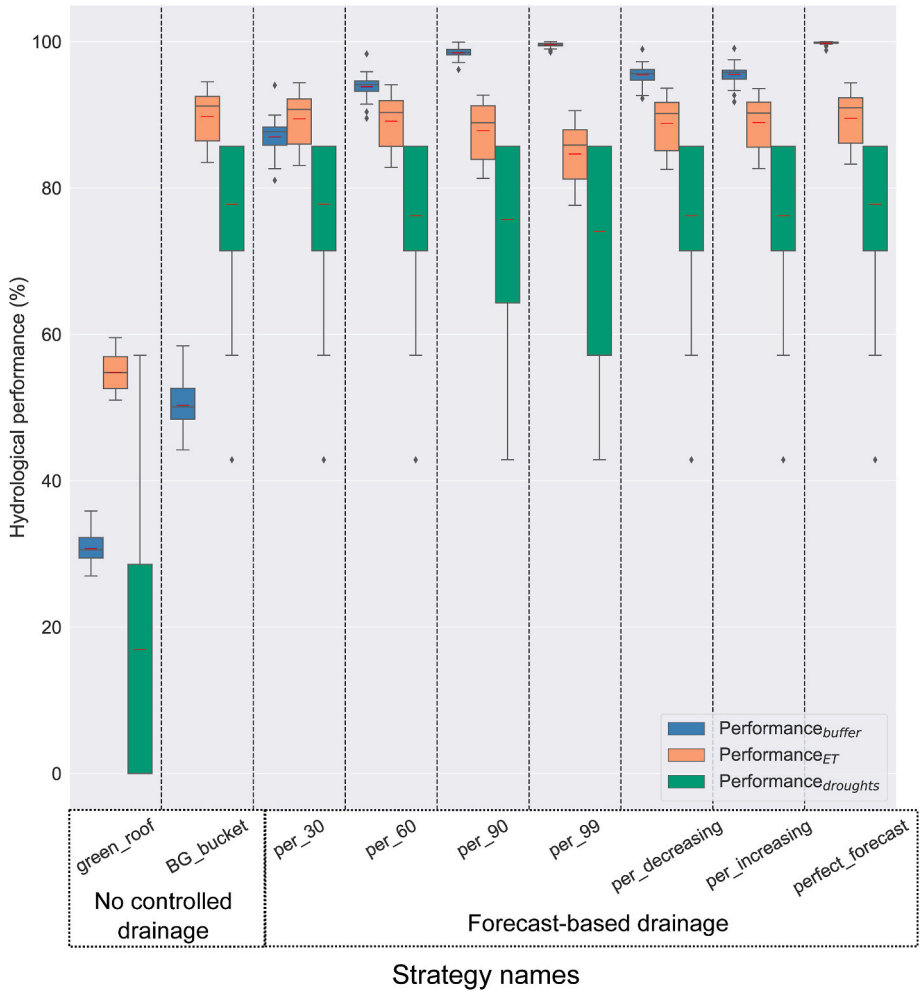

Fig. 4. The overall hydrological performance of the roof configurations, expressed as the three performance indicators for different early-drainage strategies. The boxplots represent the distributions of the performance indicators as calculated from all 27 simulated roofs. The mean values for the 27 roofs are indicated by the horizontal red lines. (For interpretation of the references to colour in this figure legend, the reader is referred to the Web version of this article.)

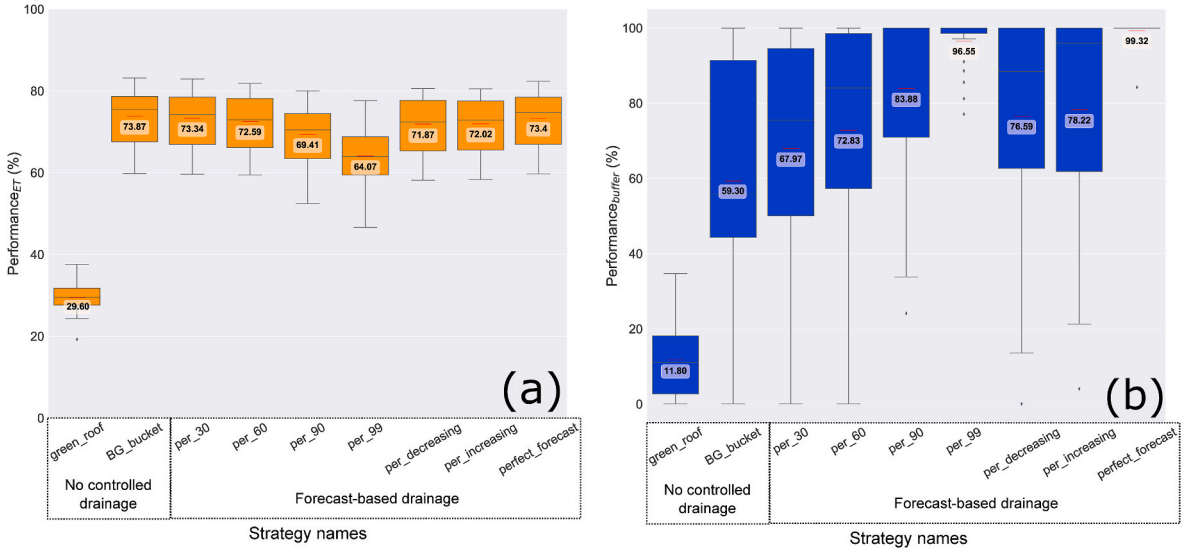

Fig. 5. Boxplots that represent the distributions of the indicators of the performance of the 27 roofs in providing evaporative cooling during summer heat events with $T > 25$ °C (Panel a) and buffer capacity during extreme rainfall events with $P > 20$ mm/h (Panel b). The numbers indicate the mean values of the performance indicators, which are represented by the red horizontal lines. (For interpretation of the references to colour in this figure legend, the reader is referred to the Web version of this article.)

strategies. The use of high percentiles from the forecast ensemble (90th or 99th percentile) sees performance approach values that are close to 100 %.

In terms of ET performance (Eq. (2), Section 2), it is evident that blue-green roofs evaporate, and thus cool, considerably more than green roofs. There is, however, little variation between the strategies: performance is always above 80 % of PET when ECMWF forecasts are used, even for the higher percentiles. Only when the highest percentile (99th percentile) is used does ET performance drop by approximately 5 percentage points. Lastly, the mean performance of the green roof on drought resistance is only 17 % (Eq. (3), Section 2), which increases to almost 80 % for the blue-green configuration. The added value of using the blue layer as an irrigation source through capillary rise is thus evident. However, the drought indicator varies significantly between the 27 locations, as reflected by the wide confidence intervals of the green boxes. The uncertainty is lower for buffer capacity performance. This indicates that almost all stations showed a similar amount of overflow relative to total precipitation.

3.2.2. Hydrological performance during extreme events

To test roof performance in specific extreme events, we filtered the time series to include only observations of extreme precipitation ($P > 20$ mm/h) and summer heat events ($T > 25$ °C). We define rainfall peaks as precipitation in excess of 20 mm in 1 h. The extreme event is then defined as the peak itself plus the rainfall at the time steps before and after the peak for which continuous rainfall is observed. The summer heat events only represent time steps for which the observed temperature is above 25 °C. We calculated Performance_{ET} (indicator for plant growth and evaporative cooling efficiency) and $\text{Performance}_{buffer}$ (indicator for rainfall storage) for these extreme events. Our results show that the blue-green roofs perform much better than green roofs for both wet and hot extremes (Fig. 5).

3.2.2.1. Summer heat events.

The average Performance_{ET} is lower for each strategy when the model is applied only to summer heat events (Fig. 5a cf Fig. 4). This stands to reason because summers are dryer than winters, while the evaporative demand of the plants is also higher in summer. Consequently, average ET effectiveness is only 74 %, even when controlled drainage is not allowed (the 'BG_bucket' configuration). The use of higher percentiles, that is, allowing more roof drainage, results in less evaporation, with an ET decrease towards 64 % for the 99th percentile. However, the drop in ET at the 90th percentile is limited, and it is only 4.5 percent points lower than under the 'BG_bucket' configuration (Fig. 5a).

3.2.2.2. Extreme rainfall events.

The 'BG_bucket' configuration already exhibits comparatively high effectiveness in storing rainfall, with a mean $\text{Performance}_{buffer}$ of 59 % (Fig. 5b). This performance increases to >83 % if the 90th and 99th percentiles are used. Some rainfall events simply exceed the capacity of the blue layer (71 mm). For this reason, performance is less than 100 % (but still 99 %) even with perfect forecasts ('perfect_strategy' configuration). The 'per_increasing' strategy yields better performance than its 'per_decreasing' counterpart. The most likely explanation is that the 'per_increasing' strategy triggers drainage for extreme events with long lead times if those events are only forecast by a small number of ensemble members. Notably, this more frequent drainage with uncertain, relatively long lead times does not result in considerably less evaporation than the other strategies (Fig. 5a). Overall, using high (90–99th) percentiles from the ECMWF ensemble precipitation forecast results in a very high capture ratio, even during extreme events.

3.3. Case-study application: suitability analysis in Amsterdam

While single blue-green roofs provide local benefits, applying them

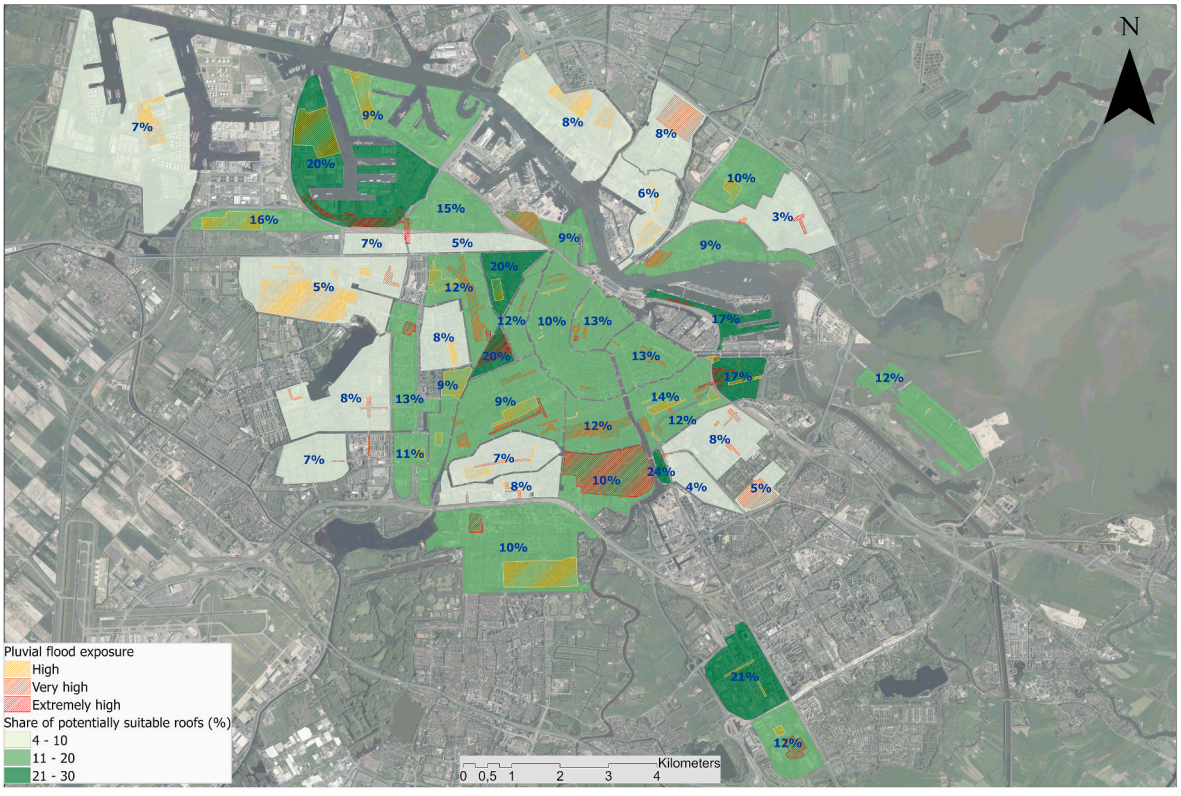

Fig. 6. A map that visualises the potential of the blue-green roof concept in Amsterdam, focusing on catchments where pluvial flooding occurs regularly (drainage bottlenecks). The blue numbers represent the share (in %) of rainfall that can potentially be captured by blue-green roofs in the catchment when the 'per_90' strategy is used. (For interpretation of the references to colour in this figure legend, the reader is referred to the Web version of this article.)

on a larger scale can reduce drainage bottlenecks and, with them, pluvial flood risk throughout the city. Fig. 6 shows the potential of blue-green roofs in Amsterdam if they are applied to all suitable roofs in the city. Assuming that suitable roofs are flat and larger than 200 m^2, we found that the total surface area of the potentially suitable roofs in Amsterdam is approximately 14 km^2 (Fig. 6), around 6.5 % of the total surface area of the municipality of Amsterdam. Fig. 6 shows the hydrological units ('catchments') that contain drainage bottlenecks. For each, pluvial flood exposure ranges from 'high' to 'extremely high' (The Municipality of Amsterdam, 2021). The bottlenecks were identified by a hydrological modelling study and expert estimates from the municipality. We calculated the share of suitable roofs for each catchment. On average, 13.3 % of the surface area of the catchments in question is potentially suitable for the implementation of blue-green roofs. Some catchments show even greater promise, with possible coverage at more than 20 % (darkest green in Fig. 6).

To determine the hydrological impact of coverage, we assumed that the average buffer performance in extreme rainfall events (>20 mm/h) from Fig. 5b is a realistic estimate of real performance. We then assumed a capture ratio of 84 % for extreme rainfall under the 'per_90' strategy. If the coverage of catchments with drainage bottlenecks is 13.3 %, roof performance can be transposed to the catchment scale. We estimate that, on average, 11 % of extreme rainfall can be captured in these urban catchments (Fig. 6, blue numbers). This 11 % capture ratio will reduce pluvial flood risk as the intensity of extreme rainfall events considered (>20 mm/h) is equal to the maximum capacity of the Amsterdam drainage system. It follows that blue-green roofs can capture a considerable amount of extreme rainfall in flood-prone catchments and that they could contribute to enhancing flood resilience in urban areas. However, an array of different flood risk reduction measures beyond (blue-)green roofs are needed to minimise damage of future extreme rainfall events (e.g. other forms of green infrastructure, retention and detention basins and expansion of drainage pipes).

4. Discussion and recommendations

4.1. Limitations of the hydrological model

In this study, we built on Cirkel et al.'s (2018) work to develop a hydrological model and to simulate the hydrological fluxes on a blue-green roof with a valve whose operation is based on precipitation forecasts. We used the evaporation module that Cirkel et al. (2018) developed. It assumes that ETa is equal to PET when water supply is abundant (>10 mm in the green layer) and that it decreases linearly for lower water contents. Cirkel et al. (2018) showed that, in comparison to ET observations measured with weighing lysimeters, their modelled ETa estimates are accurate, with a Nash-Sutcliffe Efficiency (NSE) > 0.73 and Pearson's $r > 0.86$ (see Figs. 6 and 7 in Cirkel et al., 2018). On a conventional green roof that has a limited water supply, sedum plants will shift to CAM metabolism. Evaporation will occur predominantly during the night. Accordingly, the plants will often provide only minor evaporative cooling on hot summer days. On blue-green roofs with abundant water, however, sedum maintains a C3 metabolism and therefore exhibits high daytime evaporation rates (Cirkel et al., 2018). These outcomes justify the model assumption that ETa equals PET when water levels in the green layer exceed 10 mm as well as the high summer daytime evaporation rates during heat events in our model. Other vegetation types (grasses, shrubs or trees) have even higher evaporation rates when water is abundant. However, these higher rates do not necessarily translate into improved cooling during heatwaves because more frequent dry periods in the blue and green layer are possible in such instances. Higher evaporation rates can also result in more long-term drought events, as in 2018, and even more plant deaths. This said, lower overall water levels could make these types of vegetation more effective than sedum in capturing extreme rainfall. We find that sedum vegetation, when combined with a water retention layer, already exhibits high buffer capacity. At the same time, sedum has been shown to be more drought resistant than other vegetation types (Nagase and Dunnett, 2010). Due to these reasons, we decided to omit other types of vegetation from the model.

Furthermore, the simulations cover a period of only seven years, which is too brief to be sufficiently representative of hydrological extremes. It was for this reason that we decided to use observations from 27 weather stations situated across the Netherlands. The observations capture 45 extreme precipitation events (>20 mm/h). The relatively large amount of extreme rainfall observations decrease the uncertainty of the estimated buffer capacity performance during these events. The number of droughts in the sample is much lower, but 2018 was notoriously dry. The estimated return period of this drought in the current climate is approximately 30 years (Sluijter et al., 2018). This extreme drought reduced the drought and ET performance of the roofs at every meteorological station for all early-drainage strategies. Droughts also explain why performance was considerably lower than 100 % (see Fig. 5a) even without forecast errors (Fig. 5a, 'perfect_forecast') or drainage (Fig. 5a, 'BG_bucket').

4.2. Anticipatory drainage using ECMWF forecasts

Although the forecasts of the ECMWF model perform well compared to those of other deterministic and ensemble global-scale models (Haiden et al., 2019), they are not without limitations. The 18 km grid-box average of the forecasts is an important source of errors. Observed extreme rainfall rates at certain points in the grid box can be systematically more extreme than the grid-box mean. Therefore, the ECMWF model is likely to underestimate the most extreme local events (Hewson and Pillosu, 2020). This tendency, in tandem with the extreme precipitation events that the forecast simply misses, leads to some overflow in all early-drainage strategies (Fig. 5b). However, even for these extreme events, the ECWMF ensemble precipitation forecasts can still increase the effectiveness of blue-green roofs. To increase the accuracy of forecasts at the point scale, ECWMF is developing forecasts called EcPoint (Hewson and Pillosu, 2020). These forecasts use a wholly novel statistical post-processing method to correct for bias on the grid-box scale and introduce sub-grid variability. Sub-grid variability tends to be small in cases of dynamics-driven (i.e., large-scale) rainfall and large for small-scale instability-driven convective rainfall clusters, whose size typically varies between a few hundred meters and several kilometres. At the time of writing, these forecasts with a sufficient time coverage are not yet available. However, they could be used in future studies of anticipatory water management.

The horizontal resolution of ECMWF ensemble forecasts has been 18 km since March 2016. However, between January 2010 and February 2016, it was only 35 km. As hindcasts with 18 km resolution are only run twice a week instead of twice a day, we used the historical operational archive with these original resolutions. However, we compared the two periods (2013–2016 and 2016–2019) and found no notable qualitative difference between them, as far as the added value of the forecasts for blue-green roofs is concerned. Accordingly, we decided to include the 2013–2016 period to account for a larger number of extreme events.

Every forecasting or early-warning system has inaccuracies that result in false alarms or misses. These inaccuracies can be evaluated through different metrics (e.g., the false alarm rate, the false alarm ratio or the Relative Operating Characteristic (ROC)). We did not conduct a verification analysis of the ECMWF ensemble forecasts. Instead, we evaluated them by using hydrological performance indicators. The hydrological indicators reflect the impact of inaccuracies in both the precipitation forecasts and the hydrological model on the performance of the roofs. The blue layer acts as a buffer for forecast inaccuracies: a reduction in ET only occurs when the water level in the green layer is below 10 mm, which, in turn, only occurs when the blue layer is empty. Therefore, false alarms by the ECMWF precipitation forecast and the attendant unnecessary drainage do not result in a reduction of ET

directly. The same is true of misses in the ECMWF forecasts: they do not necessarily result in overflow because extreme precipitation events usually take place in summer, when the water level in the blue layer is generally low.

An estimate of the costs of these misses and false alarms would enable the probability threshold (i.e., the percentile of the ensemble distribution) to be optimised to minimise total expense. These costs capture the consequences of water levels that are too low or too high, as indicated by the red lines in Fig. 2b. Unnecessary overflow causes flood damage. Low water levels and reduced evaporation cause higher heat stress mortality and more frequent plant deaths. The benefits of green roofs are variable and depend on many different factors (e.g. weather characteristics, the environment, roof access), as described by, among others, Manso et al. (2021) and Teotónio et al. (2021). Therefore, the optimal probability threshold will be different for every roof and in every neighbourhood. For example, a suburb with high pluvial flood risk would benefit from using high percentiles of the ECMWF ensemble precipitation distribution, whereas a central district with a high-capacity drainage system and a strong UHI effect might benefit from no or conservative drainage, which maximises evaporative cooling. Moreover, many of the benefits that are associated with (blue-)green roofs are difficult to monetise or quantify. Considerable uncertainty thus shrouds the topic (Manso et al., 2021). Due to these complexities, we decided against translating our hydrological indicators into cost-effectiveness terms. Future studies of the monetisation of the benefits of green roofs, and especially those of blue-green roofs, could consider the selection of optimal trigger thresholds by reference to cost optimisation criteria.

4.3. Effectiveness in capturing extreme rainfall events

We have evaluated the effectiveness of blue-green roofs in capturing extreme rainfall (>20 mm/h). The 27 weather stations captured 45 such events, with a mean capture ratio of 84 % using ECMWF's 90th percentile. It should be noted that the performance is generally lowest for the most extreme events. Some cloudbursts with very high accumulated rainfall are present in the observations. A precipitation event on July 28, 2014, of 131 mm in 4 h was recorded at the Deelen station (see Fig. S1 for the location), which was only captured for 30 % (using the 90th percentile) due to an underestimation in the ECMWF forecast. 11 other very extreme events were recorded (>40 mm accumulated rainfall) of which on average 70 % of rainfall was captured using ECMWF's 90th percentile. This shows that blue-green roofs can still considerably reduce runoff for these cloudbursts, although with a slightly lower performance than observed for less extreme events.

The sedum green roofs showed capture ratios of 30 % and 12 % for all rainfall events and for extreme rainfall events, respectively. The reason for the lower capture ratio of green roofs compared to blue-green roofs for all events and even more for extreme events is that rainfall intensity regularly exceeds the infiltration capacity of the soil layer on green roofs (Yao et al., 2020). These results underscore the inverse relationship between rainfall intensity and runoff retention efficiency (Liu et al., 2021). Our capture ratios (also called retention rate/-performance) for extreme rainfall are in line with the findings of Zhang et al. (2021) for green roofs with a 10-cm substrate in Beijing. Zhang et al. (2021) found capture ratios for extreme rainfall of between 5 % and 15 %. Stovin et al. (2015) found capture ratios of 15–25 % for rainfall events exceeding 20 mm of cumulative rainfall for a green roof in Sheffield. Lee et al. (2015) found similar runoff reduction rates of between 14 % and 34 % for a green roof with a 15-cm substrate. However, these latter rainfall events had an approximate intensity of only 3 mm/h, and are therefore less intense than the events analysed in our study. This said, the studies in question confirm our findings about the limited water buffer capacity of green roofs during extreme precipitation events, while that of blue-green roofs is higher.

Runoff reduction on (blue-) green roofs is also dependent on the rainfall duration and timing of the peak rainfall. Yio et al. (2013) found that an early rainfall peak can be better attenuated due to a high storage availability. Differences in these antecedent conditions, and the partly random nature of rain showers, often cause high uncertainty around retention estimates (Stovin et al., 2015). These factors partly explain the spread around the mean buffer performance among stations as shown in Figs. 4 and 5b.

4.4. Flood risk reduction on a city-scale

The suitability analysis, presented in Fig. 6, includes two main criteria: roofs should be flat, and larger than 200 m^2. Another important factor determining roof suitability is the strength, or load-bearing capacity of the roof. We did not include this factor in the analysis, because it is hard to estimate from currently available data, and requires onsite expert judgements and construction calculations. To provide an indication of the influence of building strength on the suitability analysis we explored building age as an additional criterion. Buildings built after 1960 more frequently have a concrete foundation and roof deck, increasing their load-bearing capacity and likelihood of being suitable (De Key, 2021). Adding this factor to the criteria led to a reduction of suitable roofs from 14 km^2 to 10 km^2 (Fig. S3). However, estimating the load-bearing capacity of the roof based on only building age is uncertain, and therefore we did not include it in the main results depicted in Fig. 6.

We chose the 20 mm/h threshold for extreme precipitation because it corresponds to the maximum capacity of the Amsterdam drainage system. Pluvial flooding can be expected in some parts of the city when such events occur. This impact-based threshold can differ slightly from one neighbourhood to another. Some neighbourhoods have already implemented more city greening or they have increased the capacity of the drainage system. Conversely, there may be places with a capacity below 20 mm/h. Lower capacity may be caused by blocked sewage inlets or pipes. Moreover, we currently assume that all parts of an urban catchment contribute equally to the drainage bottleneck identified by the city and, hence, that every blue-green roof in the catchment contributes to a decrease in flood risk. Hydrological 2D simulations and observations from pilot studies, however, show that the roofs that are closest to the bottlenecks have a much greater impact than more distant roofs (Van Rijn, 2020). To address these issues, future studies could develop 2D drainage modelling further and transpose the discharge reductions found in this study into spatial flood maps with estimates of flood depths and durations. Although blue-green roofs under the current strategies do not release water when it rains, a simultaneous controlled release of water from many blue-green roofs can still potentially contribute to floods at the drainage bottlenecks. Therefore, real-time observations and predictions of the available capacity of the drainage system should in future be embedded in a decision support system to further optimize water release from the roofs.

5. Conclusion and recommendations

This study has shown that blue-green roofs that operate on the basis of forecasts are effective urban climate adaptations to extreme precipitation and heat events. Installing an additional blue water retention layer underneath the green layer considerably improves the hydrological performance of traditional green roofs. Total water availability during dry and hot summers and buffer capacity during precipitation events both increase. Relatively low-resolution ECMWF precipitation forecasts further improve the performance of blue-green roofs in capturing extreme precipitation and can thus be incorporated into local anticipatory water management solutions.

We arrived at these results by testing the hydrological performance of blue-green roofs. To that end, we used a hydrological model and seven years of KNMI weather observations from 27 different locations in the Netherlands. Blue-green roofs can capture >50 % of total and extreme (>20 mm/h) rainfall without any controlled drainage through a valve.

Nevertheless, the capacity of blue-green roofs is not always high enough, and considerable overflow may occur during rainfall. Therefore, we used ECMWF ensemble precipitation forecasts to trigger controlled drainage prior to rainfall events, which greatly increases the capture ratio for total precipitation (>90 %) and for extreme precipitation (>80 %). For these capture ratios to obtain, it is necessary that drainage be based on high values of the ensemble distribution (90th or 99th percentile). This necessity inevitably leads to a minor reduction in overall water availability due to the higher influence of false alarms. Therefore, on hot summer days, the ET performance of a blue-green roof without any controlled drainage (74 % of PET) is superior to that observed under controlled drainage based on the 90th percentile of the ECMWF ensemble distribution (69 % of PET). The decrease in evaporation of around 5 percentage points translates into a reduction of evaporative cooling during heat events. The decrease is dwarfed by the gain in buffer capacity, which is around 25 percentage points. The use of very extreme forecast values (i.e., the 99th percentile) results in a capture ratio of almost 100 %, but it also causes ETa relative to PET to decline to 64 %. This serves to highlight the trade-off between the need for high water levels for evaporative cooling and roof vegetation health during droughts and the need for low water levels at the start of extreme precipitation events. Future studies should assess the capacity of (post-processed) higher-resolution or point-rainfall ensemble forecasts from ECMWF to improve forecast-based action systems further. This improvement may increase the buffer capacity of blue-green roofs for the most extreme rainfalls, and it may help to address the aforementioned trade-off between water availability and buffer capacity.

When applying the findings to the case-study for Amsterdam, we find that converting all the potentially suitable roofs to blue-green roofs would cause 11 % of extreme precipitation (>20 mm/h) in flood-prone urban catchments to be captured, provided that the 90th percentile of ECMWF ensemble forecasts is used. Evidently, the potential of blue-green roofs to mitigate pluvial flooding in Amsterdam is significant. Combined with the general results, this shows that cities implementing smart blue-green roofs with high exposure to extreme rainfall events (e.g. Amsterdam, Zurich or Jakarta) benefit from forecast-based operation of the roof's water level, and the use of high percentiles (e.g. 90th percentile) of the ECMWF precipitation ensemble distribution to increase buffer capacity. Conversely, cities in arid or semi-arid climates (e.g., Madrid, Las Vegas, Cairo) might benefit from conservative or no drainage and might need additional water sources. In addition, the use of evaporation forecasts could supplement precipitation forecasts to limit drainage when high evaporation demands are forecast. Not all cities have the same amount of flat roofs, and the roofs in some cities are not strong enough to carry a blue layer. For roofs with a sufficient construction strength, it is important to design them on future weather extremes using regional climate projections. The weather extremes of the future will increase the economic viability of a deeper water retention layer. Future studies should investigate these upscaling conditions, including their institutional, social and financial dimensions, in Amsterdam and beyond.

Author contributions

Tim Busker: Conceptualization, Methodology, Software, Writing – Original Draft, Review & Editing, Visualization. Hans de Moel: Conceptualization, Methodology, Writing – Review & Editing, Supervision. Toon Haer: Conceptualization, Methodology, Writing – Review & Editing, Supervision, Project administration. Maurice Schmeits: Methodology, Writing – Review & Editing, Supervision. Bart van den Hurk: Conceptualization, Methodology, Writing – Review & Editing, Supervision. Kira Myers: Software, Methodology, Writing – Review & Editing. Dirk Gijsbert Cirkel: Software, Methodology, Writing – Review & Editing. Jeroen Aerts: Conceptualization, Resources, Writing - Review & Editing, Project administration, Funding acquisition.

Declaration of competing interest

The authors declare that they have no known competing financial interests or personal relationships that could have appeared to influence the work reported in this paper.

Acknowledgements

This work is based on data from ECMWF and TIGGE, retrieved using the Meteorological Archival and Retrieval System (MARS). TIGGE (The Interactive Grand Global Ensemble) is an initiative of the World Weather Research Programme (WWRP). The research is funded by RESILIO; RESILIO is an acronym for 'Resilience nEtwork of Smart Innovative cLImate-adapative rOoftops', a collaboration between the Municipality of Amsterdam, Waternet, MetroPolder company, Rooftop Revolution, HvA, VU, Stadgenoot, de Alliantie and De Key. This project is co-financed by the European Regional Development Fund through the Urban Innovative Actions Initiative. We would like to thank MetroPolder company, in particular Merle van der Kroft and Joost Jacobi, for their help and support during this research project. In addition, we would like to thank ECWMF User Services for the excellent support on the use of ECMWF ensemble forecasts.

Appendix A. Supplementary data

Supplementary data to this article can be found online at https://doi.org/10.1016/j.jenvman.2021.113750.

References

Aflaki, A., Mirnezhad, M., Ghaffarianhoseini, Amirhosein, Ghaffarianhoseini, Ali, Omrany, H., Wang, Z.H., Akbari, H., 2017. Urban heat island mitigation strategies: a state-of-the-art review on Kuala Lumpur, Singapore and Hong Kong. Cities 62, 131–145. https://doi.org/10.1016/J.CITIES.2016.09.003.

Alexandri, E., Jones, P., 2008. Temperature decreases in an urban canyon due to green walls and green roofs in diverse climates. Build. Environ. 43, 480–493. https://doi.org/10.1016/j.buildenv.2006.10.055.

Allen, R.G., Pereira, L.S., Raes, D., Smith, M., et al., 1998. Crop Evapotranspiration-Guidelines for Computing Crop Water Requirements-FAO Irrigation and Drainage Paper 56, vol. 300. Fao, Rome, D05109.

Andenæs, E., Time, B., Muthanna, T., Asphaug, S., Kvande, T., 2021. Risk reduction framework for blue-green roofs. Buildings 11, 185. https://doi.org/10.3390/buildings11050185.

Bougeault, P., Toth, Z., Bishop, C., Brown, B., Burridge, D., De Chen, H., Ebert, B., Fuentes, M., Hamill, T.M., Mylne, K., Nicolau, J., Paccagnella, T., Park, Y.Y., Parsons, D., Raoult, B., Schuster, D., Dias, P.S., Swinbank, R., Takeuchi, Y., Tennant, W., Wilson, L., Worley, S., 2010. The thorpex interactive grand global ensemble. Bull. Am. Meteorol. Soc. https://doi.org/10.1175/2010BAMS2853.1.

Buizza, R., Richardson, D., 2017. 25 years of ensemble forecasting at ECMWF|ECMWF (No. 153). ECMWF Newsl. https://doi.org/10.21957/bv418o.

Chan, F.K.S., Griffiths, J.A., Higgitt, D., Xu, S., Zhu, F., Tang, Y.T., Xu, Y., Thorne, C.R., 2018. "Sponge City" in China—a breakthrough of planning and flood risk management in the urban context. Land Use Pol. 76, 772–778. https://doi.org/10.1016/j.landusepol.2018.03.005.

Cirkel, D.G., Voortman, B.R., van Veen, T., Bartholomeus, R.P., 2018. Evaporation from (Blue-)Green roofs: assessing the benefits of a storage and capillary irrigation system based on measurements and modeling. Water 10. https://doi.org/10.3390/w10091253.

De Key, 2021. Personal Email Communication.

Dutch government, 2021. Basisregistratie Adressen en Gebouwen (BAG). https://data.overheid.nl/en/dataset/basisregistratie-adressen-en-gebouwen–bag-. (Accessed 15 March 2021).

Dutch government, 2017. Actueel Hoogtebestand Nederland (AHN3). https://downloads.pdok.nl/ahn3-downloadpage/. (Accessed 11 March 2021).

ECMWF, 2021. The ECMWF Web API. https://www.ecmwf.int/en/forecasts/access-forecasts/ecmwf-web-api. (Accessed 28 May 2021).

ESRI, 2021. Multivariate Clustering (Spatial Statistics)—ArcGIS Pro | Documentation. https://pro.arcgis.com/en/pro-app/latest/tool-reference/spatial-statistics/multivariate-clustering.htm#GUID-4CF323C1-9117-42A8-BAD1-A06CC2CACB83. (Accessed 11 June 2021).

Gravatt, D.A., Martin, C.E., 1992. Comparative ecophysiology of five species of Sedum (Crassulaceae) under well-watered and drought-stressed conditions. Oecologia 92, 532–541. https://doi.org/10.1007/BF00317845.

Haiden, T., Janousek, M., Vitart, F., Ferranti, L., Prates, F., 2019. Evaluation of ECMWF Forecasts, Including the 2019 Upgrade. ECMWF.

Hewson, T.D., Pillosu, F.M., 2020. A New Low-Cost Technique Improves Weather Forecasts across the World (arXiv).
Huang, Y., Tian, Z., Ke, Q., Liu, J., Irannezhad, M., Fan, D., Hou, M., Sun, L., 2020. Nature-based solutions for urban pluvial flood risk management. WIREs Water 7. https://doi.org/10.1002/wat2.1421.
Imhoff, R.O., Brauer, C.C., Overeem, A., Weerts, A.H., Uijlenhoet, R., 2020. Spatial and temporal evaluation of radar rainfall nowcasting techniques on 1,533 events. Water Resour. Res. 56 https://doi.org/10.1029/2019WR026723.
Indlekofer, H., Rouve, G., 1975. Discharge over polygonal weirs. J. Hydraul. Div. 101, 385–401. https://doi.org/10.1061/jyceaj.0004226.
IPCC, 2021. Summary for policymakers. In: Masson-Delmotte, V., Zhai, P., Pirani, A., Connors, S.L., Péan, C., Berger, S., Caud, N., Chen, Y., Goldfarb, L., Gomis, M.I., Huang, M., Leitzell, K., Lonnoy, E., Matthews, J.B.R., Maycock, T.K., Waterfield, T., Yelekçi, O., Yu, R., Zhou, B. (Eds.), Climate Change 2021: The Physical Science Basis. Contribution of Working Group I to the Sixth Assessment Report of the Intergovernmental Panel on Climate Change. Cambridge University Press. In Press.
Ireson, A.M., Butler, A.P., 2013. A critical assessment of simple recharge models: application to the UK Chalk. Hydrol. Earth Syst. Sci. 17, 2083–2096. https://doi.org/10.5194/hess-17-2083-2013.
Jackson, R.D., Idso, S.B., Reginato, R.J., Pinter, P.J., 1981. Canopy temperature as a crop water stress indicator. Water Resour. Res. 17, 1133–1138. https://doi.org/10.1029/WR017i004p01133.
Kellert, S.R., Calabrese, E.F., 2015. The Practice of Biophilic Design. Biophilic-Design.com.
KNMI, 2021. Klimatologie - Metingen en waarnemingen. https://www.knmi.nl/nederland-nu/klimatologie-metingen-en-waarnemingen. (Accessed 18 May 2021).
Kuronuma, T., Watanabe, H., 2017. Photosynthetic and transpiration rates of three Sedum species used for green roofs. Environ. Control Biol. 55, 137–141. https://doi.org/10.2525/ecb.55.137.
La Roche, P., Berardi, U., 2014. Comfort and energy savings with active green roofs. Energy Build. 82, 492–504. https://doi.org/10.1016/j.enbuild.2014.07.055.
Lee, J.Y., Lee, M.J., Han, M., 2015. A pilot study to evaluate runoff quantity from green roofs. J. Environ. Manag. 152, 171–176. https://doi.org/10.1016/j.jenvman.2015.01.028.
Liu, W., Engel, B.A., Feng, Q., 2021. Modelling the hydrological responses of green roofs under different substrate designs and rainfall characteristics using a simple water balance model. J. Hydrol. 602, 126786 https://doi.org/10.1016/J.JHYDROL.2021.126786.
Manola, I., Van Den Hurk, B., De Moel, H., Aerts, J.C.J.H., 2018. Future extreme precipitation intensities based on a historic event. Hydrol. Earth Syst. Sci. 22, 3777–3788. https://doi.org/10.5194/hess-22-3777-2018.
Manso, M., Teotónio, I., Silva, C.M., Cruz, C.O., 2021. Green roof and green wall benefits and costs: a review of the quantitative evidence. Renew. Sustain. Energy Rev. https://doi.org/10.1016/j.rser.2020.110111.
MetroPolder company, 2021a. MetroPolder Company: the Polder of the City. https://metropolder.com/en/. (Accessed 31 August 2021).
MetroPolder company, 2021b. Personal Email Communication.
Mohajerani, A., Bakaric, J., Jeffrey-Bailey, T., 2017. The urban heat island effect, its causes, and mitigation, with reference to the thermal properties of asphalt concrete. J. Environ. Manag. 197, 522–538. https://doi.org/10.1016/j.jenvman.2017.03.095.
Monteith, J., Unsworth, M., 2013. Principles of Environmental Physics: Plants, Animals, and the Atmosphere. Academic Press.
Nagase, A., Dunnett, N., 2010. Drought tolerance in different vegetation types for extensive green roofs: effects of watering and diversity. Landsc. Urban Plann. 97, 318–327. https://doi.org/10.1016/j.landurbplan.2010.07.005.
Pelorosso, R., Petroselli, A., Apollonio, C., Grimaldi, S., 2021. Blue-green roofs: hydrological evaluation of a case study in Viterbo, Central Italy. In: Lecture Notes in Civil Engineering. Springer, Cham, pp. 3–13. https://doi.org/10.1007/978-3-030-68824-0_1.
Penman, H.L., 1948. Natural evaporation from open water, hare soil and grass. Proc. R. Soc. Lond. A. Math. Phys. Sci. 193 https://doi.org/10.1098/rspa.1948.0037.
Pilon-Smits, E.A.H., 't Hart, H., Meesterburrie, J.A.N., Naber, P., Kreuler, R., Van Brederode, J., 1991. Variation in crassulacean acid metabolism within the genus Sedum: carbon isotope composition and water status dependent phosphoenolpyruvate carboxylase activity. J. Plant Physiol. 137, 342–346. https://doi.org/10.1016/S0176-1617(11)80143-4.
Razzaghmanesh, M., Beecham, S., Salemi, T., 2016. The role of green roofs in mitigating Urban Heat Island effects in the metropolitan area of Adelaide, South Australia. Urban For. Urban Green. 15, 89–102. https://doi.org/10.1016/j.ufug.2015.11.013.
Redactie Rainproof, 2020. Wolkbreuk 28 Juli 2014. https://www.rainproof.nl/wolkbreuk-28-juli. (Accessed 20 November 2020).
RESILIO, 2020. Smart Blue-Green Roofs. https://resilio.amsterdam/en/smart-blue-green-roofs/. (Accessed 10 November 2020).
Shafique, M., Kim, R., Lee, D., 2016. The potential of green-blue roof to manage storm water in urban areas. Nat. Environ. Pollut. Technol. 15, 715–718.
Skjeldrum, P.M., Kvande, T., 2017. Moisture-resilient upgrading to blue-green roofs. Energy Procedia. https://doi.org/10.1016/j.egypro.2017.09.649.
Skougaard Kaspersen, P., Høegh Ravn, N., Arnbjerg-Nielsen, K., Madsen, H., Drews, M., 2017. Comparison of the impacts of urban development and climate change on exposing European cities to pluvial flooding. Hydrol. Earth Syst. Sci. 21, 4131–4147. https://doi.org/10.5194/hess-21-4131-2017.
Sluijter, R., Plieger, M., van Oldenborgh, G.J., Beersma, J., de Vries, H., 2018. De Droogte Van 2018: Een Analyse Op Basis Van Het Potentiële Neerslagtekort.
Stovin, V., Vesuviano, G., De-Ville, S., 2015. Defining green roof detention performance, pp. 574–588. https://doi-org.vu-nl.idm.oclc.org/10.1080/1573062X.2015.1049279. https://doi.org/10.1080/1573062X.2015.1049279, 14.
Swinbank, R., Kyouda, M., Buchanan, P., Froude, L., Hamill, T.M., Hewson, T.D., Keller, J.H., Matsueda, M., Methven, J., Pappenberger, F., Scheuerer, M., Titley, H. A., Wilson, L., Yamaguchi, M., 2016. The TIGGE project and its achievements. Bull. Am. Meteorol. Soc. https://doi.org/10.1175/BAMS-D-13-00191.1.
Teotónio, I., Silva, C.M., Cruz, C.O., 2021. Economics of green roofs and green walls: a literature review. Sustain. Cities Soc. 69, 102781 https://doi.org/10.1016/j.scs.2021.102781.
The municipality of Amsterdam, 2021. Rainproof bottleneck map. https://maps.amsterdam.nl/rainproof/?LANG=en. (Accessed 23 April 2021).
Tzoulas, K., Korpela, K., Venn, S., Yli-Pelkonen, V., Kaźmierczak, A., Niemela, J., James, P., 2007. Promoting ecosystem and human health in urban areas using Green Infrastructure: a literature review. Landsc. Urban Plann. 81, 167–178. https://doi.org/10.1016/J.LANDURBPLAN.2007.02.001.
van den Berg, M., Wendel-Vos, W., van Poppel, M., Kemper, H., van Mechelen, W., Maas, J., 2015. Health benefits of green spaces in the living environment: a systematic review of epidemiological studies. Urban For. Urban Green. 14, 806–816. https://doi.org/10.1016/j.ufug.2015.07.008.
Van den Hurk, B., Siegmund, P., Tank, A.K., Attema, J., Bakker, A., Beersma, J., Bessembinder, J., Boers, R., Brandsma, T., Van Den Brink, H., Drijfhout, S., Eskes, H., Haarsma, R., Hazeleger, W., Jilderda, R., Katsman, C., Lenderink, G., Loriaux, J., Van Meijgaard, E., Van Noije, T., Van Oldenborgh, G.J., Selten, F., Siebesma, P., Sterl, A., De Vries, H., Van Weele, M., De Winter, R., Van Zadelhoff, G., 2014. KNMI ' 14 : Climate Change Scenarios for the 21st Century – A Netherlands Perspective. Sci. Rep. WR2014-01, KNMI, De Bilt, The Netherlands. www.climatescenarios.nl.
Van Oldenborgh, G.J., Lenderink, G., 2014. Een eerste blik op de buien van maandag 28 juli 2014. Meteorologica 3, 28–29.
Van Rijn, A., 2020. The Hydrological Impact of Blue-Green Roofs in Amsterdam: a Model-Based Case Study for Slotermeer and the Rivierenbuurt (MSc Thesis). Vrije Universiteit Amsterdam (VU).
Van Woert, N.D., Rowe, D.B., Andresen, J.A., Rugh, C.L., Xiao, L., 2005. Watering regime and green roof substrate design affect Sedum plant growth. Hortscience 40, 659–664. https://doi.org/10.21273/hortsci.40.3.659.
Viavattene, C., Ellis, J.B., 2013. The management of urban surface water flood risks: SUDS performance in flood reduction from extreme events. Water Sci. Technol. 67, 99–108. https://doi.org/10.2166/wst.2012.537.
Waternet, Tauw, 2017. Vlakkenkaart Amsterdam, Amsterdam.
World Meteorological Organization (WMO), 2021. Summer of Extremes: Floods, Heat and Fire. https://public.wmo.int/en/media/news/summer-of-extremes-floods-heat-and-fire. (Accessed 9 August 2021).
World Weather Attribution (WWA), 2021. Western North American Extreme Heat Virtually Impossible without Human-Caused Climate Change. https://www.worldweatherattribution.org/western-north-american-extreme-heat-virtually-impossible-without-human-caused-climate-change/. (Accessed 1 September 2021).
World Wildlife Fund (WWF), 2016. Natural and Nature-Based Flood Management: a Green Guide. Washington, DC.
Yao, L., Wu, Z., Wang, Y., Sun, S., Wei, W., Xu, Y., 2020. Does the spatial location of green roofs affects runoff mitigation in small urbanized catchments? J. Environ. Manag. 268, 110707 https://doi.org/10.1016/j.jenvman.2020.110707.
Yio, M.H.N., Stovin, V., Werdin, J., Vesuviano, G., 2013. Experimental analysis of green roof substrate detention characteristics. Water Sci. Technol. 68, 1477–1486. https://doi.org/10.2166/wst.2013.381.
Zhang, Shouhong, Lin, Z., Zhang, Sunxun, Ge, D., 2021. Stormwater retention and detention performance of green roofs with different substrates: observational data and hydrological simulations. J. Environ. Manag. 291, 112682 https://doi.org/10.1016/j.jenvman.2021.112682.